NUCL SCI TECH (2017) 28:124
DOI 10.1007/s41365-017-0280-1

Sequence-dependent interactions between model peptides and lipid bilayers

Hao-Zhi Lei[1,2] · Tian Tian[1] · Qiqige Du[3] · Jun Hu[1] · Yi Zhang[1]

Received: 10 January 2017 / Revised: 22 February 2017 / Accepted: 27 February 2017 / Published online: 5 August 2017

Abstract Studying interaction between peptides and lipid membranes is helpful for understanding the working mechanism of amyloidogenic peptides and antimicrobial peptides, which are toxic to cells through disruption of the cell membrane. Although many efforts have been made to find out common mechanisms of the peptide-induced membrane disruption, detailed information on how the peptide's amino acid sequence affects its interaction with lipid bilayers is still lacking. In this study, three peptides termed as Pep11, P11-2, and QQ11, which share a similar backbone, were employed to explore how modifications on the peptide sequence as well as terminal groups influenced its interaction with the lipid membrane. Atomic force microscopy data revealed that the peptides could deposit on the membranes and induce defects with varied morphologies and stiffness. Fluorescence resonance energy transfer (FRET) experiments indicated that the introduction of the three peptides resulted in different FRET effects on either liquid or gel lipid membranes. DPH fluorescence anisotropy and Laurdan's generalized polarization analysis showed that P11-2 could insert into the lipid membrane and impact the lipid hydrophobic region while QQ11 influenced the order of the hydrophilic head of the lipid membrane. With these results, we have illustrated how these peptides interacted differently with the lipid membrane because of the modification of their sequences. Although these peptides did not relate to disease and antibiosis, we hope these results still could provide some clues for partly understanding the working mechanism of amyloidogenic peptides and antimicrobial peptides.

Keywords Peptides · Lipid membrane · Atomic force microscopy · Fluorescence methods

1 Introduction

Amyloidogenic peptides (AMYs) and antimicrobial peptides (AMPs) have the ability to interact with cells and induce cytotoxicity [1–3]. A large number of studies have pointed out that these peptides interact with cells through the disruption of cell membrane [4–7]. Several models have been proposed to understand the membrane disruption induced by the peptides, in which the peptides could bind, insert, and destroy the cytomembrane [8–11] via a multiple-effect process [12]. Lipid bilayers have been a good model system for investigating the interactions between peptides and the cell membrane [4, 13]. For examples, Lal and Yu [14] found that amyloid-like peptides could insert supported lipid bilayers (SLBs) to form ion channels, and they speculated that the ion channels would induce cell degeneration and pathophysiology. Galvagnion et al. [15] found that lipid vesicles induced the nucleation of α-synuclein and initiated the peptides aggregation.

This work was supported by the National Basic Research Program of China (973 program) (No. 2013CB932801), and the National Natural Science Foundation of China (Nos. 11274334 and 11374205).

✉ Yi Zhang
zhangyi@sinap.ac.cn

[1] Key Laboratory of Interfacial Physics and Technology, Shanghai Institute of Applied Physics, Chinese Academy of Sciences, Shanghai 201800, China

[2] University of Chinese Academy of Sciences, Beijing 100049, China

[3] School of Life Sciences, Inner Mongolia Agricultural University, Hohhot 010018, China

Many methods and tools can be used to explore the interactions of lipid bilayers and peptides [16]. Atomic force microscopy (AFM), which has a high spatial resolution and has been widely used for studying biomaterials [17–20], is a powerful tool for investigating SLBs [21, 22] as well as various phenomenon happening on it [23, 24]. Fluorescence resonance energy transfer (FRET) with two related fluorescent probes has shown the ability to exhibit changes of membranes fluidity and lipid reorganization [25]. The two probes, 1,6-diphenyl-1,3,5-hexatriene (DPH) as a fat-soluble fluorescence dye [26] and Laurdan as a hydrophilic dye [27], reveal the interaction sites of peptide molecules on the lipid bilayers through changes of fluorescence anisotropy and generalized polarization. These methods and tools could provide details about the interactions between peptides and lipid bilayers ingeniously.

Although excellent achievements have been made, detailed information on how the peptide's amino acid sequence [28–30] affects its interaction with lipid bilayers is still lacking. However, this kind of information is crucial for understanding the working mechanism of AMYs and AMPs for its further applications.

In order to get more insight into the sequence-dependent interactions between lipid membranes and peptides, we planned to employ three model peptides that share a similar sequence consisting of 11 amino acid residues (Fig. 1). The peptide termed as P11-2 contains two hydrophilic residues (Arg and Glu) and two aromatic residues (Phe and Trp), which was previously shown to self-assemble into fibrillary structures [31–35]. Previous studies indicated that P11-2 could form pores and insert into a model membrane as an Aβ protein. So it is a good model to study the interaction between peptides and lipid membrane [36]. The other two peptides were originated from P11-2. The terminal-deacetylated P11-2 was termed as Pep11 [34]. The last one was named as QQ11, in which two hydrophilic residuals (Arg) in Pep11 were replaced with Phe so that it became more hydrophobic than P11-2 and Pep11. From previous work, these peptides could form β-sheet conformation and self-assemble into nanofilaments on a mica substrate [31, 34].

In this paper, AFM, FRET, and fluorescence analysis data displayed that the replacement of hydrophilic amino acid residuals with hydrophobic ones and adding/taking off

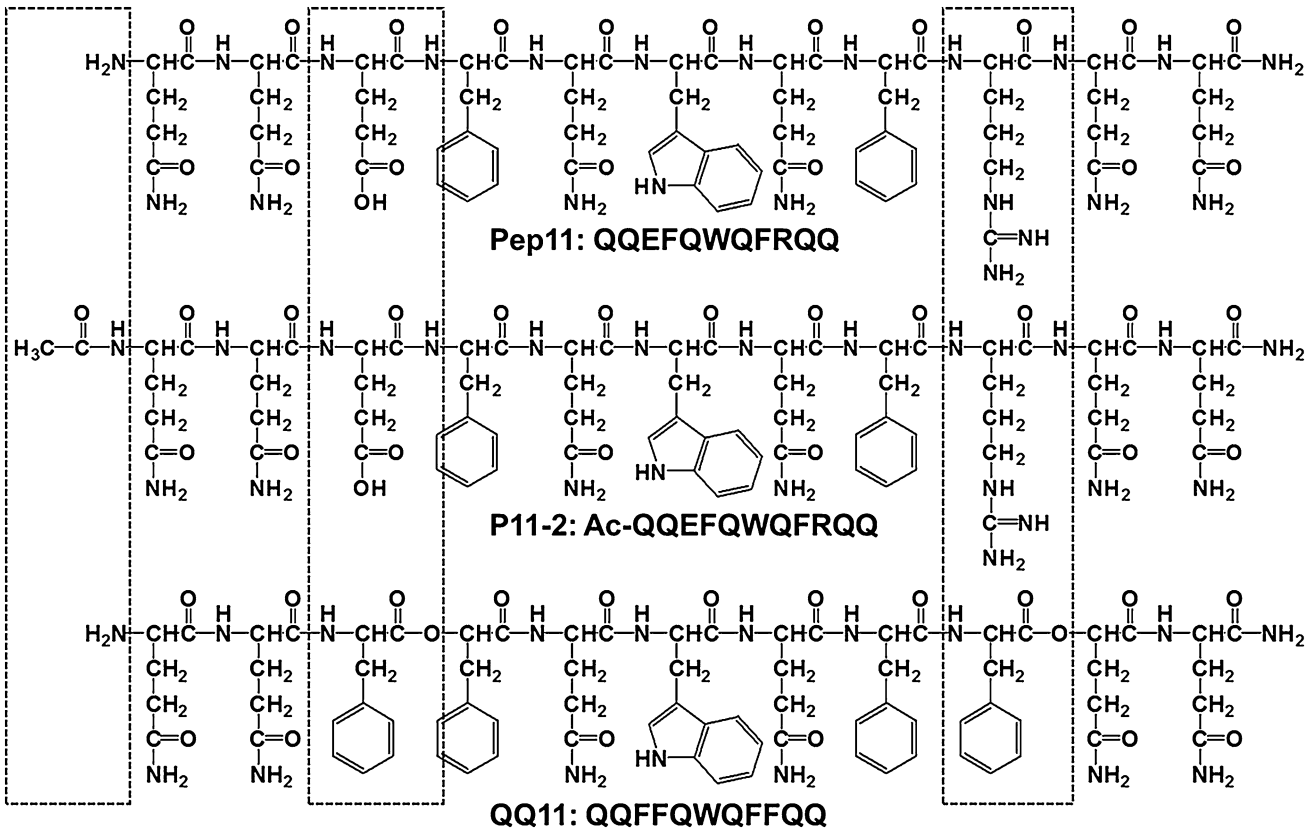

Fig. 1 Scheme drawing illustrating the molecular sequences of peptides that were used in this paper. The differences in the sequences of these model peptides are highlighted with *dashed rectangles*. The peptides were acetylated at the *C* ends so that their properties were close to the natural proteins [37]

the hydrophobic cap of a peptide would affect its interaction with the lipid bilayers differently. The results showed that these modifications on the peptide sequences would result in morphologically and/or mechanically different defects on the SBLs as well as changes in its effective locations in the lipid bilayers. In addition, it was found that the liquid-phase lipid membrane responds in a quite different way to the gel-phase lipid membrane upon adding peptides to them.

2 Materials and methods

2.1 Materials

P11-2 (>95%), Pep11 (>95%), and QQ11 (>95%) were synthesized by the Chinese Peptide Company. 1,2-dioleoyl-sn-glycerol-3-phosphocholine (DOPC), 1,2-dipalmitoyl-sn-glycero-3-phosphocholine (DPPC), 1,2-dimyristoyl-sn-glycero-3-phosphoethanolamine-*N*-(lissamine rhodamine B sulfonyl) (N-Rh-PE), and 1,2-dimyristoyl-sn-glycerol-3-phosphoethanolamine-*N*-(7-nitro-2-1,3-benzoxadiazol-4-yl) (N-NBD-PE) were purchased from Avanti Polar Lipids. 6-dodecanoyl-2-dimethylaminonaphthalene (Laurdan) and 1-(4-trimethylammoniumphenyl)-6-Phenyl-1,3,5-Hexatriene *p*-Toluenesulfonate (TMA-DPH) were obtained from Life Technologies. 1,6-diphenyl-1,3,5-hexatriene (DPH), Thioflavin T (ThT), and other reagents used in this work were purchased from Sigma-Aldrich.

2.2 Preparation of peptide and lipid bilayers

The peptide was dissolved in pure water. The peptide solution was centrifuged at 14,000 rpm (Hitachi Koki Co., Ltd.) for 15 min at 4 °C, and the supernatant was used immediately. The final concentrations were 0.5 and 0.05 mM for Pep11, 0.15 and 0.015 mM for DN1, and 0.03 and 0.003 mM for QQ11, respectively.

The preparation of small unilamellar vesicles (SUVs) followed previously reported procedures [21, 38]. Briefly, DPPC and DOPC were dissolved in chloroform with a mole proportion of 1:1. Then, the mixture was thoroughly dried by blowing nitrogen gas for more than 4 h. Finally, pure water was added to the dry mixture, and the suspension was ultrasonicated for 4 h in a 25 °C bath sonication. The final concentration of lipid vesicles in the experiments was 0.65 mM.

After dropping 10 μL $CaCl_2$ aqueous solution (20 mM) onto a freshly cleaved mica substrate (1 cm × 1 cm), the 50 μL DOPC/DPPC vesicle solution was added on the mica substrate as well. About 2 min later, the mica substrate was washed with a sufficient amount of water to remove excessive vesicles which did not form SLBs. Finally, the peptide solution was added onto the SLBs and incubated for 10 min. After that, the sample was washed with a large amount of water again to remove the excessive peptide.

2.3 Atomic force microscopy (AFM)

The morphology and mechanical properties of the peptide–SLBs composites were studied with AFM in fluid. The Multimode AFM system (Nanoscope 8, Bruker) equipped with a J scanner was used. The PeakForce quantitative nanomechanics (PF-QNM) mode was also adopted for mechanical property study. Silicon nitride cantilevers, with tips of about 10 nm in radius (DNP-S, 0.35 N m^{-1}, Bruker), were used. Before imaging, the AFM probe was cleaned for 1 min by a plasma cleaner (Harrick Plasma) [39]. In PF-QNM experiments, the deflection sensitivity of the cantilever was calibrated on mica in pure water and the spring constant of the cantilever was obtained from Thermal Tune.

2.4 Fluorescence resonance energy transfer (FRET)

The FRET experiment was followed by the procedures reported in the literature [25]. Prior to being dried by nitrogen gas, a chloroform solution of DOPC/DPPC was mixed with two fluorescent-modified lipids, N-NBD-PE and N-Rh-PE, with a mole ratio of 1:1:250:250 (N-NBD-PE:N-Rh-PE:DOPC:DPPC). After the fluorescently labeled lipid vesicles were prepared in water, they were put into a black 96-well plate, and the fluorescent emissions at 538 and 590 nm were measured by a Thermo Scientific Fluoroskan Ascent (Thermo Fisher Scientific) at 25 °C by using 460 nm as excitation. The FRET efficiency was calculated from the following equation: $e = (R_i - R_{100\%})/(R_0 - R_{100\%}) \times 100$, where R represents the fluorescence intensity ratio at 538 nm (N-NBD-PE emission)/590 nm (N-Rh-PE emission), R_i represents the fluorescence emission ratios of peptide/vesicles and vesicles only, and R_0 represents the fluorescence intensity ratio which is the value collected from a mixture of 20% Triton X-100 and vesicles [25].

2.5 DPH fluorescence anisotropy

DPH was dissolved in 98% ethanol and used as the stock solution. After mixing DPH with lipid vesicles (final concentration of DPH was 6 μM), peptides were added into dye-labeled lipid vesicles. 10 min later, the fluorescence anisotropy of the samples were measured by an F-4500 fluorescence spectrophotometer (Hitachi Koki Co., Ltd.)

under temperature ranging from 10 to 60 °C. The excitation wavelength was 355 nm while the emission wavelength was 430 nm [26]. Anisotropy values (r) were calculated by the following equation: $r = (I_{VV} - G \times I_{VH})/(I_{VV} + 2 \times G \times I_{VH})$, where G was the inherent factor that could be obtained from equipment when measured and I_{VV} and I_{VH} were the fluorescence intensities measured in directions 0° and 90° [40].

2.6 Laurdan's generalized polarization (GP)

Lipid vesicles were prepared following the above-mentioned procedures. Then, Laurdan was mixed with lipid vesicles to a final concentration of 4 μM. After that peptides were mixed with the dye-labeled lipid vesicles. 10 min later, the fluorescence intensities were measured on an F-4500 fluorescence spectrophotometer (Hitachi Koki Co., Ltd.) under temperature ranging from 10 to 60 °C. The excitation wavelength was 350 nm, while the emission wavelength varied between 365 and 550 nm. The GP is calculated by the following equation: $GP = (I_{440} - I_{490})/(I_{440} + I_{490})$, where I_{440} and I_{490} were fluorescence intensities at the wavelength 440 and 490 nm, respectively [41].

2.7 ThT fluorescence assay

The peptide QQ11 solution (0.003 mM) with ThT (final concentration 20 nM) was added into a black 96-well plate and detected by a Thermo Scientific Fluoroskan Ascent (Thermo Fisher Scientific) at 25 °C. The excitation wavelength was 440 nm while the emission wavelength was 485 nm. The fluorescence intensity was measured every 5 min for 60 min [34].

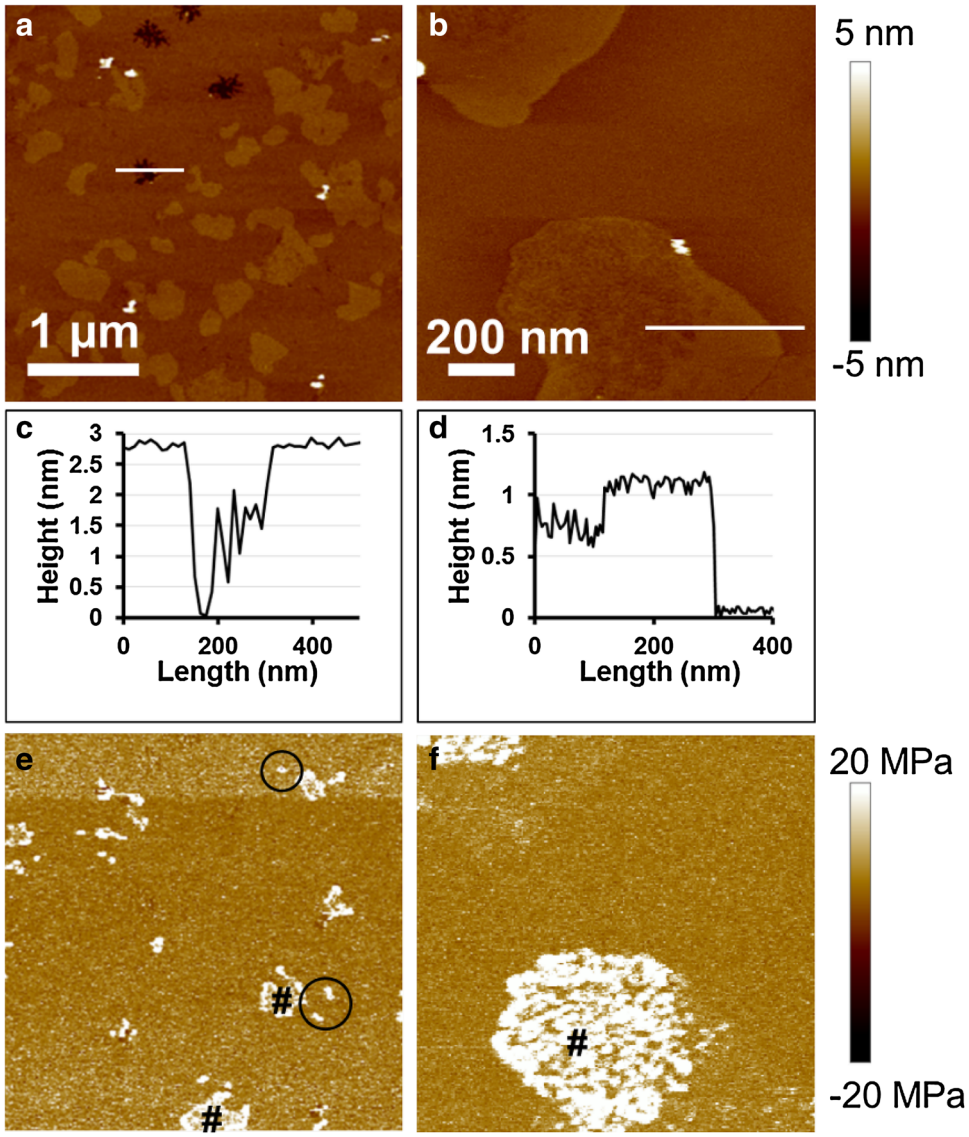

Fig. 2 (Color online) The AFM morphology images and mechanical analysis of the Pep11 and SLBs composites. **a**, **b** Height images indicating Pep11 on SLBs and **c**, **d** corresponding section analysis of the *white lines*. **e**, **f** Young's modulus images corresponds to **a** and **b**, respectively. The *black pounds* and *circles* in **e, f** highlighted the Young's modulus of defect areas

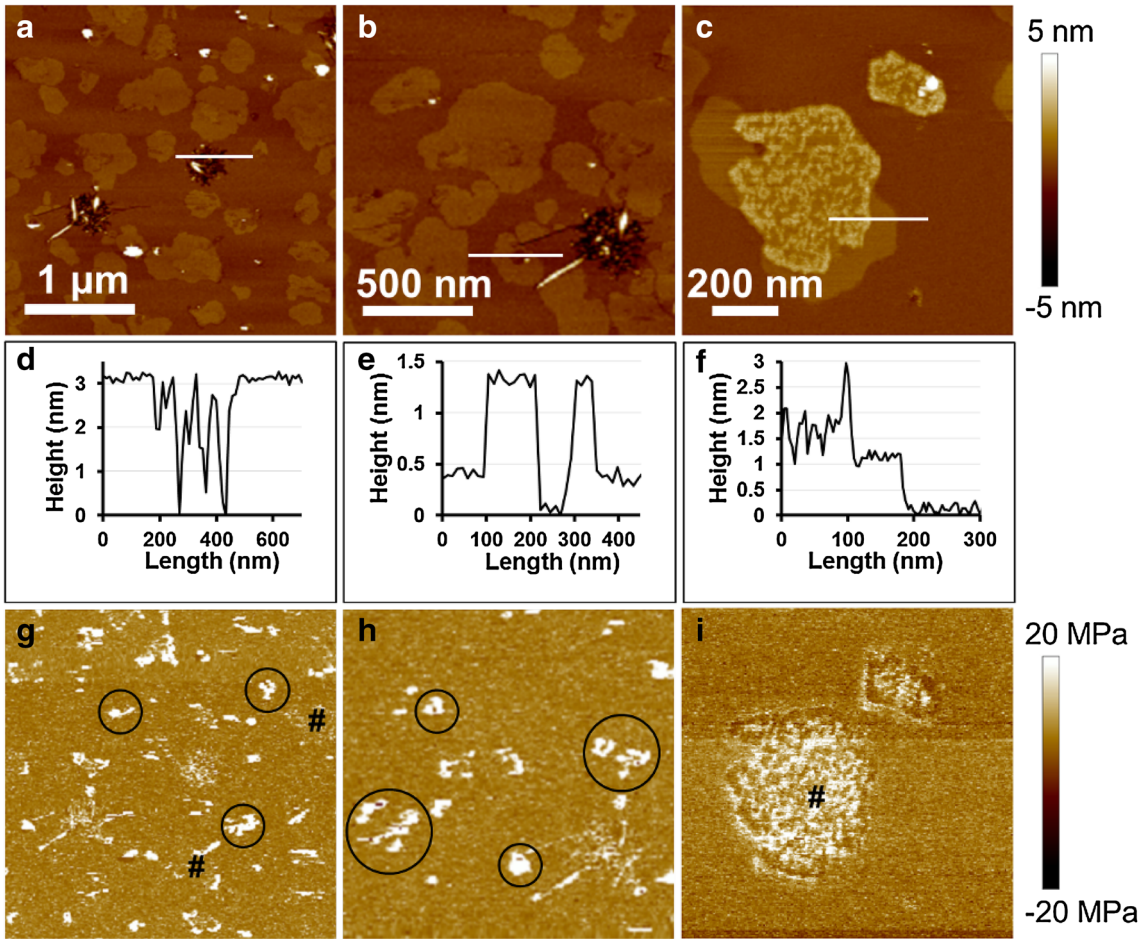

Fig. 3 (Color online) The AFM morphology images and mechanical analysis of the composites of P11-2 and SLBs. **a**–**c** AFM height images and **d**–**f** corresponding section analysis of the *white lines* highlighted in the AFM images. **g**–**i** Young's modulus images corresponding to **a**–**c**, respectively

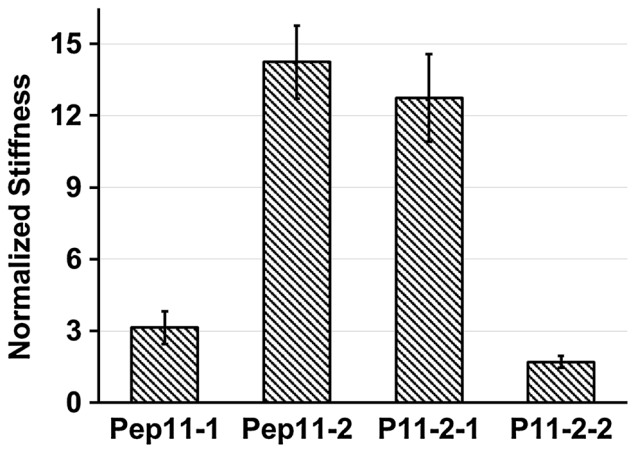

Fig. 4 Stiffness of defects on SLBs induced by peptides. The stiffness values were normalized to the Young's modulus value of normal SLBs on mica in water

3 Results and discussion

From AFM data, it was found that Pep11 could induce the formation of several kinds of defects on both liquid and gel phases of the DPPC/DOPC SLBs that are normally very smooth and uniform (Fig. 2). Section analysis exhibits that there were defects of 1–3 nm in depth in the liquid phase of SLBs (Fig. 2a), while the defects on gel domains were 0.2–0.4 nm lower than surroundings (Fig. 2b). Besides the modifications in morphology, treatment with Pep11 also resulted in changes of the mechanical properties of the SLBs. The defects on the gel phase normally had a higher Young's modulus value (marked with # in Fig. 2e–f and termed as Pep11-1). The defects on the liquid phase at 1–3 nm in depth had no detectable change in Young's modulus value; however, on liquid-phase SLBs we did find another kind of defects, which showed only ~0.2 nm in

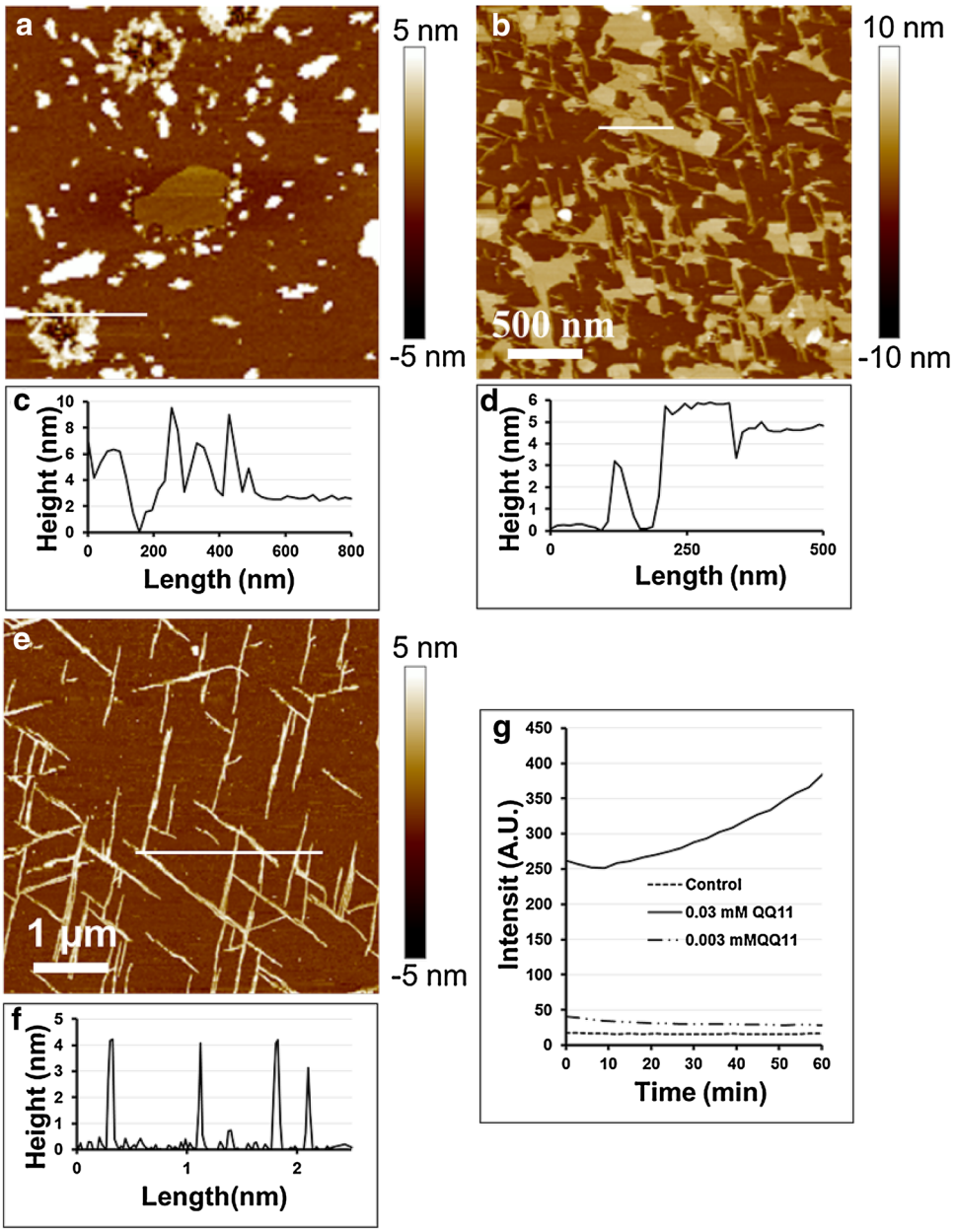

Fig. 5 (Color online) The AFM morphology images and ThT fluorescence assay. **a**–**d** AFM height images (*upper*) and corresponding section analysis (*bottom*) of the *white lines* highlighted in the AFM images. **a**, **c** QQ11 concentration 0.03 mM. **b**, **d** QQ11 concentration 0.003 mM. **e**, **f** Tapping mode AFM image (*upper*) and section analysis (*bottom*) of QQ11 (0.003 mM in water) self-assembly on mica. **g** The ThT fluorescence assay of QQ11

depth, but has a higher Young's modulus value (marked with circle in Fig. 2e and termed as Pep11-2). These results indicated that Pep11 could not only damage lipid membrane, but also impact its stiffness.

Figure 3 shows the AFM data that SLBs were interfered with P11-2. Since there is an acetyl group on the N-terminal of P11-2, it should become more hydrophobic than Pep11 so that a different impact on the SLBs was expected. The P11-2 also induced defects at 1–3 nm in depth on SLBs as well (Fig. 3a), and the defect area showed much higher Young's modulus. Careful inspection indicated that there were fibril-like structures in the defects. The increase in Young's modulus on 1–3 nm-deep defects might be a result of the fibril-like structures which were formed from P11-2. There were two other kinds of defects (highlighted with a black circle and #, respectively, in Fig. 3g–i) which also showed higher Young's modulus than normal lipid membrane. In one case (highlighted with black circle in Fig. 3h, named as P11-2-1), the defects were ~1.5 nm lower than the lipid membrane and existed on both gel and liquid state SLBs. In another case (highlighted with # in Fig. 3i, termed as P11-2-2), it only appeared on gel domains. From a high-resolution AFM image (Fig. 3c), it was found that the defects were 1–2 nm higher (Fig. 3i) than the original gel domain. P11-2-2 was similar with the defects induced by Pep11 (Fig. 2b), but were higher in morphology. From Fig. 3g, it is clear that P11-2-1 was stiffer than DN-2. The

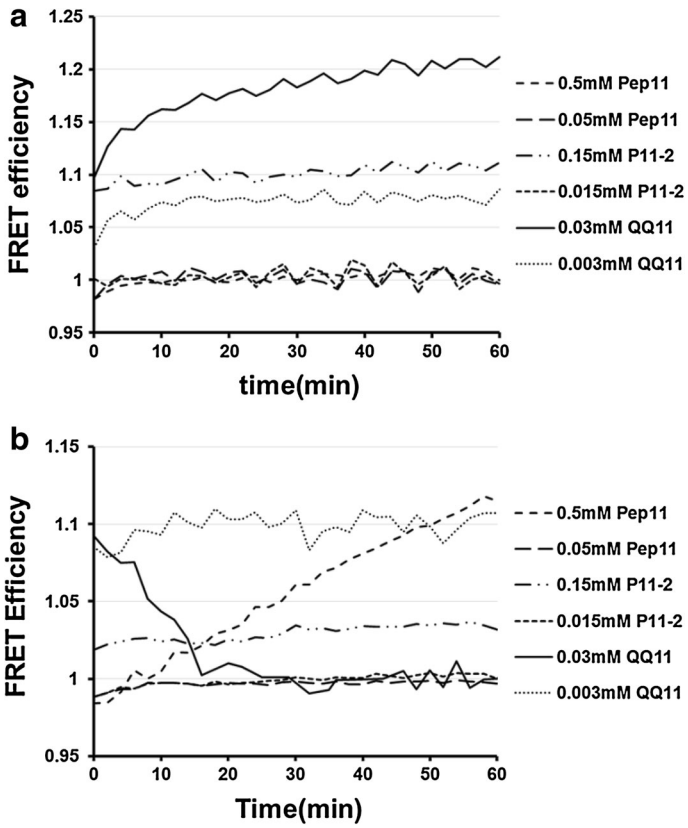

Fig. 6 FRET efficiency curves showing the effect of Pep11, P11-2, and QQ11 on lipid membranes. **a** FRET efficiency of peptides on a liquid-phase membrane. **b** FRET efficiency of peptides on a gel-phase membrane

Young's module values in different defects can be found in Fig. 4, which clearly indicates that adding the acetyl group on the *N*-terminal of the Pep11 peptide brought different effect on SLBs. The results of P11-2 are partially consistent with former research [36], which found that P11-2 could form pores and insert into lipid membranes. Unfortunately, the origin of the stiffness difference has not been understood. We speculate that it may be a result of the different interaction behaviors between the peptides and the lipid membranes involved by the variation in peptide sequences.

In the case of QQ11, it was found that QQ11 interacted with the SLBs in a different way. The effect of QQ11 on the SLBs was heavily related to its concentration. At a high QQ11 concentration (e.g., 0.03 mM), defects could be observed on the SLBs (Fig. 5a). What is more, QQ11 would aggregate on SLBs, especially around the defects (Fig. 5a, c). Interestingly, at a lower concentration of QQ11 (e.g., 0.003 mM), the QQ11 peptide could induce the lipid molecules to detach from the mica substrate while it self-assembled into nanofilamental structures on mica (Fig. 5b, d). The height of the nanofilament was $\sim$3 nm (Fig. 5b, d), which is in good agreement with the peptide nanofilament formed on a bare mica substrate (Fig. 5e, f). During the experiment, it was found that QQ11 was easy to absorb to our AFM tip (DNP-S), even if the tip was cleaned by plasma cleaner. So the correct Young's modulus image was not obtained.

It is interesting to figure out why the concentration of QQ11 affects its interaction with the SLBs. To this end, ThT fluorescence was analyzed during QQ11 self-assembling in the presence of SUVs (Fig. 5g). The result indicated that, in the QQ11 solution with a concentration of 0.03 mM, ThT had already showed relatively high fluorescence intensity even at the beginning of collecting data, while in the QQ11 solution with a concentration of 0.003 mM the ThT fluorescence intensity kept closing to that of control. This means that the QQ11 had already aggregated before data could be recorded of the ThT fluorescent intensity under a high-concentration condition, but it did not aggregate in the solution at a low concentration. As a result, aggregated QQ11 might deposit on the SLBs (Fig. 5a). In the case of QQ11 with a concentration of 0.003 mM, the peptide might detach the SLBs from the mica substrate and self-assemble on the substrate (Fig. 5b) with a substrate-assisted mechanism (as judged from the threefold symmetry of the QQ11 filaments) even in a concentration lower than its critical micelle concentration [42, 43].

From above AFM data, we found that the three model peptides indeed induced different phenomenons on SLBs. However, how these peptides impacted the SLBs and why

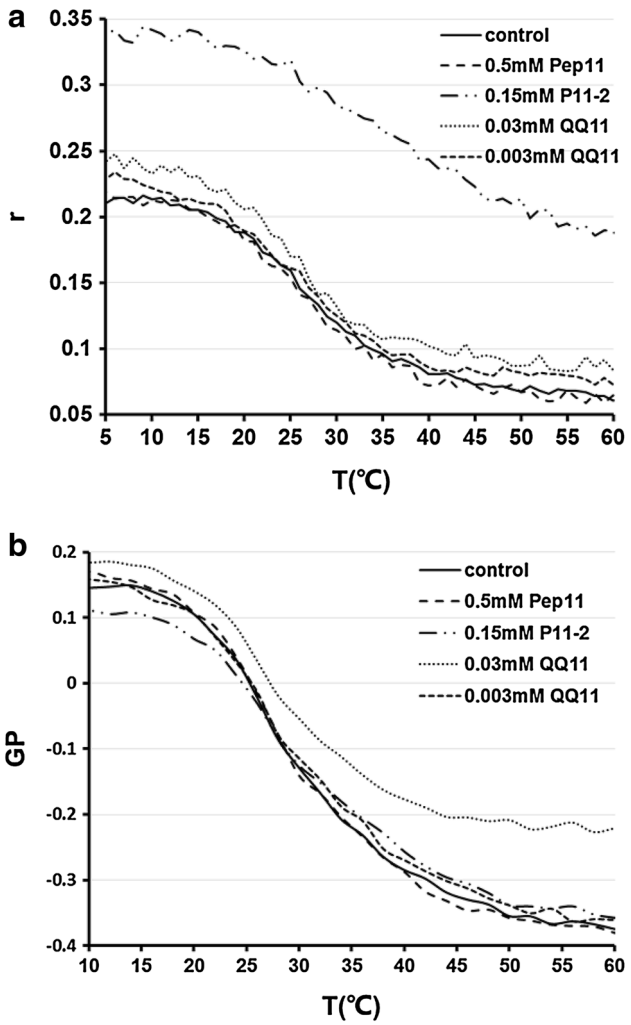

Fig. 7 Curves of DPH fluorescence anisotropy values (*r*) **a** and Laurdan's GP **b** in the presence of the peptides in the mixed liquid/gel lipid membrane

the Young's modulus of SLBs changed could not be explained by the AFM data directly. Hence, FRET and fluorescence analysis were carried out for a better understanding of these interesting AFM results.

The FRET experiments shown in Fig. 6 brought us new information that revealed how the peptides interacted with lipid membranes. The FRET experiments were based on the following design: A pair of fluorescence molecules, which are N-NBD-PE (donor) and N-Rh-PE (acceptor), normally show the FRET effect if they are in an effectively short distance. When peptides were added into the fluorescence-labeled lipid vesicles, the distance of the fluorescent donor and acceptor would be changed due to the interaction between the peptide and membrane, resulting in the change of the FRET efficiency [25]. Experiment results indicate that the three peptides show different effects on FRET with either liquid (Fig. 6a) or gel (Fig. 6b) lipid membranes. It was found that Pep11 did not influence the FRET efficiency of the liquid membrane (Fig. 6a); however, it could increase the FRET efficiency of the gel-phase membrane at high concentration (Fig. 6b). In addition, Fig. 6 showed that peptide P11-2 could increase the FRET efficiencies of both liquid- and gel-phase membranes at high concentration. In the case of QQ11, it could increase the FRET efficiencies of liquid-phase membranes. For gel-phase membranes, it was found that its effect on membranes was related to its concentration. At high concentration of QQ11, the FRET efficiency was enhanced at first, but it decreased gradually to no obvious changes. At low concentration of QQ11, the FRET efficiency maintained enhancing. The above results indicate that increase in FRET efficiency only happened in some specific cases. Once an increase in the FRET efficiency was observed, it implies that the peptide could insert into lipid membrane and make the lipid molecules closer to each other.

To further figure out the locations that the peptides bind to the lipid membranes, DPH fluorescence anisotropy and Laurdan's generalized polarization (GP) were analyzed. As a fat-soluble dye, DPH could sense changes of the hydrophobic region of lipid membranes [44]. In the DPH fluorescence anisotropy experiment, if a peptide interferes with the hydrophobic region of a lipid membrane, the fluorescence anisotropy curve would change along with the increasing of temperature. Similarly, Laurdan's GP experiment was a useful tool to study the interaction between peptides and the hydrophilic head of lipid membrane [45]. Laurdan is a dye that can bind to the hydrophilic region of lipid membrane [44]. Laurdan's GP would be changed if peptides interact with the hydrophilic head of the lipid molecules consisting of the membrane.

Figure 7a shows that fluorescence anisotropy of DPH increased significantly by introducing P11-2 into the lipid membrane while the introduction of Pep11 had no obvious changes of DPH fluorescence anisotropy. It means that P11-2 could insert into the lipid membrane, impact the lipid hydrophobic region [36], and reduce the fluidity of the membrane, while the Pep11 could not. Although QQ11 is more hydrophobic than the other two peptides, as judged from their sequences, and thus should tend to combine with the hydrophobic tails of the lipid membrane, only a slight increase in fluorescence anisotropy of DPH was observed (Fig. 7a). We guess that the hydrophobic QQ11 is difficult to pass through the hydrophobic lipid membrane, so that QQ11 could only slightly influence the hydrophobic tails of the lipid membrane.

Figure 7b illustrated that high-concentration QQ11 increased the Laurdan's GP while P11-2 and Pep11 did not. It means that QQ11 influenced the order of the hydrophilic head of the lipid membrane while Pep11 and P11-2 had no effect upon the hydrophilic head of lipid membrane. This

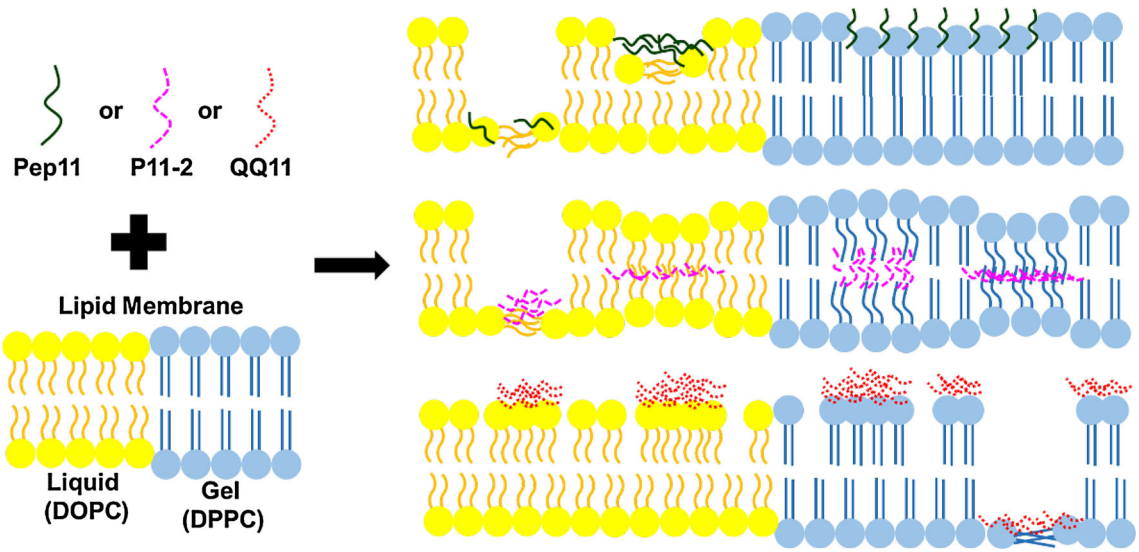

Fig. 8 (Color online) Schematic drawing illustrating the interaction between peptides and lipid membrane

result implies that only QQ11 could aggregate on the hydrophilic head of the lipid membrane, forming defects and damaging the membrane at last. It is very curious that, as shown in Fig. 2, Pep11 seemed to insert into the hydrophilic head region. However, the Laurdan's GP experiment indicated that Pep11 could not change the order of the hydrophilic head of lipid membrane. We speculated that, because of the two charged amino acids in Pep11, it could embed in the hydrophilic region of the membrane, but maintain the lipid molecules ordered structure.

By combining the results obtained from AFM, FRET, and fluorescent analysis, we illustrated a general scene of the interactions between three model peptides and lipid membranes (Fig. 8). It seems that Pep11 could embed into the lipid membrane and form defects on it, while the remaining membrane still maintains its order. The increased stiffness of SLBs maybe originate from the insertion of Pep11 so that the lipid membrane is packing tighter. In the case of P11-2, it has the ability to insert into the hydrophobic region of the lipid membrane, thus the lipid molecules are disordered and the lipid membranes are damaged. Moreover, the insertion of P11-2 occupies the space of hydrophobic tails of lipid molecules so that the tails are packing tighter and the stiffness of SLBs increases. QQ11 is the most hydrophobic one in the three peptides and is easy to aggregate in solution. The QQ11 aggregates might deposit on the lipid membranes. Because of the hydrophilic head of lipid membrane, QQ11 is hard to penetrate through the lipid membrane. However, once it penetrates through the membrane, they may assemble with each other with the assistant of the mica substrate, resulting in detachment of the SLBs from the substrate.

4 Conclusion

In summary, we studied the interactions between three model peptides and lipid membranes by means of AFM, FRET, and fluorescence analysis. AFM data revealed that the peptides could deposit on the membranes and induce defects with varied morphologies and stiffness. FRET experiments indicated that the introduction of the three peptides resulted in different FRET effects on either liquid or gel lipid membranes. DPH fluorescence anisotropy and Laurdan's generalized polarization analysis revealed that P11-2 could insert into the lipid membrane and impact the lipid hydrophobic region while QQ11 influenced the order of the hydrophilic head of the lipid membrane. These results showed that the peptides interacted differently with the lipid membrane because of the modification of their sequences. Although these peptides did not relate to disease and antibiosis, we hope these results will be helpful for understanding the working mechanisms of AMYs and AMPs and with the future design of biologically active peptides.

References

1. C.M. Dobson, Protein misfolding, evolution and disease. Trends Biochem. Sci. **24**, 329–332 (1999). doi:10.1016/s0968-0004(99)01445-0
2. M.Z. Zhang, J. Zhao, J. Zheng, Molecular understanding of a potential functional link between antimicrobial and amyloid peptides. Soft Matter **10**, 7425–7451 (2014). doi:10.1039/c4sm00907j
3. T. Tian, J.C. Zhang, H.Z. Lei et al., Synchrotron radiation X-ray fluorescence analysis of Fe, Zn and Cu in mice brain associated

with Parkinson's disease. Nucl. Sci. Tech. **26**, 030506 (2015). doi:10.13538/j.1001-8042/nst.26.030506
4. A. Quist, L. Doudevski, H. Lin et al., Amyloid ion channels: a common structural link for protein-misfolding disease. Proc. Natl. Acad. Sci. USA **102**, 10427–10432 (2005). doi:10.1073/pnas.0502066102
5. R. Kayed, Y. Sokolov, B. Edmonds et al., Permeabilization of lipid bilayers is a common conformation-dependent activity of soluble amyloid oligomers in protein misfolding diseases. J. Biol. Chem. **279**, 46363–46366 (2004). doi:10.1074/jbc.C400260200
6. A.A. Stromstedt, L. Ringstad, A. Schmidtchen et al., Interaction between amphiphilic peptides and phospholipid membranes. Curr. Opin. Colloid Interface **15**, 467–478 (2010). doi:10.1016/j.cocis.2010.05.006
7. R.E.W. Hancock, A. Patrzykat, Clinical development of cationic antimicrobial peptides: from natural to novel antibiotics. Curr. Drug Target Infect. Disord. **2**, 79–83 (2002). doi:10.2174/1568005024605855
8. S.M. Butterfield, H.A. Lashuel, Amyloidogenic protein membrane interactions: mechanistic insight from model systems. Angew. Chem. Int. Ed. **49**, 5628–5654 (2010). doi:10.1002/anie.200906670
9. M. Mustata, R. Capone, H. Jang et al., K3 fragment of amyloidogenic β2-microglobulin forms ion channels: implication for dialysis related amyloidosis. J. Am. Chem. Soc. **131**, 14938–14945 (2009). doi:10.1021/Ja9049299
10. R.M. Epand, R.F. Epand, Lipid domains in bacterial membranes and the action of antimicrobial agents. Biochim. Biophys. Acta **1788**, 289–294 (2009). doi:10.1016/j.bbamem.2008.08.023
11. R.G. Panchal, M.L. Smart, D.N. Bowser et al., Pore-forming proteins and their application in biotechnology. Curr. Pharm. Biotechnol. **3**, 99–115 (2002). doi:10.2174/1389201023378418
12. M. Tanaka, Y. Komi, Layers of structure and function in protein aggregation. Nat. Chem. Biol. **11**, 373–377 (2015). doi:10.1038/nchembio.1818
13. C.M. Yip, A.A. Darabie, J. McLaurin, Aβ 42-peptide assembly on lipid bilayers. J. Mol. Biol. **318**, 97–107 (2002). doi:10.1016/s0022-2836(02)00028-1
14. R. Lal, L. Yu, Atomic force microscopy of cloned nicotinic acetylcholine receptor expressed in *xenopus* oocytes. Proc. Natl. Acad. Sci. USA **90**, 7280–7284 (1993). doi:10.1073/pnas.90.15.7280
15. C. Galvagnion, A.K. Buell, G. Meisl et al., Lipid vesicles trigger α-synuclein aggregation by stimulating primary nucleation. Nat. Chem. Biol. **11**, 229–234 (2015). doi:10.1038/nchembio.1750
16. L.C. Salay, M. Ferreira, O.N. Oliveira Jr. et al., Headgroup specificity for the interaction of the antimicrobial peptide tritrpticin with phospholipid Langmuir monolayers. Colloid Surf. B **100**, 95–102 (2012). doi:10.1016/j.colsurfb.2012.05.002
17. D.M. Czajkowsky, H. Iwamoto, T.L. Cover et al., The vacuolating toxin from helicobacter pylori forms hexameric pores in lipid bilayers at low PH. Proc. Natl. Acad. Sci. USA **96**, 2001–2006 (1999). doi:10.1073/pnas.96.5.2001
18. J.K.H. Horber, M.J. Miles, Scanning probe evolution in biology. Science **302**, 1002–1005 (2003). doi:10.1126/science.1067410
19. D. Fotiadis, S. Scheuring, S.A. Muller et al., Imaging and manipulation of biological structures with the AFM. Micron **33**, 385–397 (2002). doi:10.1016/S0968-4328(01)00026-9
20. H.Z. Lei, X.Q. Zhang, J. Hu et al., Self-assembly of amyloid-like peptides at interfaces investigated by atomic force microscopy. Sci. Adv. Mater. **9**, 65–76 (2017). doi:10.1166/sam.2016.2737
21. M.P. Mingeot-Leclercq, M. Deleu, R. Brasseur et al., Atomic force microscopy of supported lipid bilayers. Nat. Protoc. **3**, 1654–1659 (2008). doi:10.1038/nprot.2008.149
22. L. Picas, F. Rico, S. Scheuring, Direct measurement of the mechanical properties of lipid phases in supported bilayers. Biophys. J. **102**, L1–L3 (2012). doi:10.1016/j.bpj.2011.11.4001
23. S. Scheuring, J. Seguin, S. Marco et al., Nanodissection and high-resolution imaging of the *Rhodopseudomonas viridis* photosynthetic core complex in native membranes by AFM. Proc. Natl. Acad. Sci. USA **100**, 1690–1693 (2003). doi:10.1073/pnas.0437992100
24. J. Zhong, W.F. Zheng, L.X. Huang et al., PrP106-126 amide causes the semi-penetrated poration in the supported lipid bilayers. Biochim. Biophys. Acta **1768**, 1420–1429 (2007). doi:10.1016/j.bbamen.2007.03.003
25. N. Gal, A. Morag, S. Kolusheva et al., Lipid bilayers significantly modulate cross-fibrillation of two distinct amyloidogenic peptides. J. Am. Chem. Soc. **135**, 13582–13589 (2013). doi:10.1021/ja4070427
26. B.R. Lentz, Use of fluorescent probes to monitor molecular order and motions within liposome bilayers. Chem. Phys. Lipids **64**, 99–116 (1993). doi:10.1016/0009-3084(93)90060-g
27. S.S. Antollini, M.A. Soto, I. Bonini de Romanelli et al., Physical state of bulk and protein-associated lipid in nicotinic acetylcholine receptor-rich membrane studied by laurdan generalized polarization and fluorescence energy transfer. Biophys. J. **70**, 1275–1284 (1996). doi:10.1016/S0006-3495(96)79684-4
28. A. Won, A. Ruscito, A. Ianoul, Imaging the membrane lytic activity of bioactive peptide latarcin 2a. Biochim. Biophys. Acta **1818**, 3072–3080 (2012). doi:10.1016/j.bbamem.2012.07.030
29. M. Bucciantini, E. Giannoni, F. Chiti et al., Inherent toxicity of aggregates implies a common mechanism for protein misfolding diseases. Nature **416**, 507–511 (2002). doi:10.1038/416507a
30. J.D. Savoie, F. Otis, J. Burck et al., Crown ether helical peptides are preferentially inserted in lipid bilayers as a transmembrane ion channels. Biopolymers **104**, 427–433 (2015). doi:10.1002/bip.22633
31. C. Whitehouse, J.Y. Fang, A. Aggeli et al., Adsorption and self-assembly of peptides on mica substrates. Angew. Chem. Int. Ed. **44**, 1965–1968 (2005). doi:10.1002/anie.200462160
32. A. Aggeli, M. Bell, L.M. Carrick et al., PH as a trigger of peptide β-sheet self-assembly and reversible switching between nematic and isotropic phases. J. Am. Chem. Soc. **125**, 9619–9628 (2003). doi:10.1021/ja021047i
33. A. Aggeli, M. Bell, N. Boden et al., Responsive gels formed by the spontaneous self-assembly of peptides into polymeric β-sheet tapes. Nature **386**, 259–262 (1997). doi:10.1038/386259a0
34. Q.Q.G. Du, B. Dai, J.H. Hou et al., A comparative study on the self-assembly of an amyloid-like peptide at water–solid interfaces and in bulk solutions. Microsc. Res. Tech. **78**, 375–381 (2015). doi:10.1002/jemt.22483
35. A. Aggeli, I.A. Nyrkova, M. Bell et al., Hierarchical self-assembly of chiral rod-like molecules as a model for peptide beta-sheet tapes, ribbons, fibrils, and fibers. Proc. Natl. Acad. Sci. USA **98**, 11857–11862 (2001). doi:10.1073/pnas.191250198
36. L.C. Salay, W. Qi, B. Keshet et al., Membrane interactions of a self-assembling model peptide that mimics the self-association, structure and toxicity of Aβ(1–40). Biochim. Biophys. Acta **1788**, 1714–1721 (2009). doi:10.1016/j.bbamem.2009.04.010
37. B. Maillère, M. Hervé, The specificity of antibodies raised against AT cell peptide is influenced by peptide amidation. Mol. Immunol. **34**, 1003–1009 (1997). doi:10.1016/S0161-5890(97)00121-1
38. H.Z. Lei, X.J. Zhou, H.X. Wu et al., Morphology change and detachment of lipid bilayers from the mica substrate driven by graphene oxide sheets. Langmuir **30**, 4678–4683 (2014). doi:10.1021/la500788z
39. Y. Song, B.Y. Zhao, L.J. Zhang et al., The origin of the "snap-In" in the force curve between AFM probe and the water/gas

interface of nanobubbles. ChemPhysChem **15**, 492–499 (2014). doi:10.1002/cphc.201301081
40. J.H. Nyström, M. Lönnfors, T.K.M. Nyholm, Transmembrane peptides influence the affinity of sterols for phospholipid bilayers. Biophys. J. **99**, 526–533 (2010). doi:10.1016/j.bpj.2010.04.052
41. T. Sheynis, A. Friediger, W.F. Xue et al., Aggregation modulators interfere with membrane interactions of β2-microglobulin fibrils. Biophys. J. **105**, 745–755 (2013). doi:10.1016/j.bpj.2013.06.015
42. F. Zhang, H.N. Du, Z.X. Zhang et al., Epitaxial growth of peptide nanofilaments on inorganic surfaces: effects of interfacial hydrophobicity/hydrophilicity. Angew. Chem. Int. Ed. **45**, 3611–3613 (2006). doi:10.1002/anie.200503636
43. S.G. Kang, T. Huynh, Z. Xia et al., Hydrophobic interaction drives surface-assisted epitaxial assembly of amyloid-like peptides. J. Am. Chem. Soc. **135**, 3150–3157 (2013). doi:10.1021/ja310989u
44. H. Pruchnik, D. Bonarska-Kujawa, H. Kleszczynska, Effect of chlorogenic acid on the phase transition in phospholipid and phospholipid/cholesterol membranes. J. Am. Chem. Soc. **118**, 943–950 (2014). doi:10.1007/s10973-014-3841-0
45. A.R. Vaughn, T.A. Bell, E. Gibbons et al., Relationships between membrane water molecules and Patman equilibration kinetics at temperatures far above the phosphatidylcholine melting point. Biochim. Biophys. Acta **1848**, 942–950 (2015). doi:10.1016/j.bbamem.2014.12.021